Environmental Science and Pollution Research (2020) 27:38384–38396
https://doi.org/10.1007/s11356-019-06995-x

Characterization of Tagaran natural clay and its efficiency for removal of cadmium (II) from Sulaymaniyah industrial zone sewage

Bakhtyar K. Aziz[1] · Dler M. Salh Shwan[2] · Stephan Kaufhold[3]

Received: 15 August 2019 / Accepted: 7 November 2019 / Published online: 7 December 2019

Abstract

The fine fraction of the Tagaran natural clay (TC) from the Kurdistan region of Iraq-Sulaimani was characterized and used to remove Cd ions from industrial swage. Using XRF, XRD, SEM, and FTIR, the dominant clay mineral of the Tagaran clay mineral was identified as saponite, with minor amounts of chlorite. The clay was examined for its efficiency to adsorb and remove (Cd^{2+}) in the presence of other heavy metal contaminants from Sulaimani industrial zone sewage by a batch method. The effect of initial pH, equilibrium time, temperature, clay dosage, and Cd^{2+} concentration was studied. Results were evaluated using Langmuir, Freundlich, Temkin, and Redlich-Peterson isotherms. The kinetics could be best fitted to pseudo-second-order reaction kinetic model. In addition, the activation energy and the amount of calculated and experimentally determined heavy metal loads were consistent. The thermodynamic studies showed spontaneous endothermic adsorption. The trioctahedral smectite (saponite) showed a good efficiency for the adsorption of Cd^{2+} from the real sample (up to 100%) which at least partly can be explained by cation exchange. Tagaran clay is a candidate material for the production of an adsorber material for removing Cd^{2+} from aqueous solutions.

Keywords Tagaran natural clay · Cadmium · Isotherm · Sewage · Saponite

Introduction

Cadmium is one of the heavy metals widely utilized in the industry although it is known to be toxic. Cadmium is used for the production of Ni-Cd batteries, printing inks, electroplating, and pigments for paints, plastics, rubber, lacquers, and special alloys. Natural cadmium ores occur in association with Zinc ore (Hwang and Wang 2001) (Vig et al. 2003) (Chamsaz et al. 2013). Cadmium accumulates in the human's body, especially in the kidneys and liver (Roushani et al. 2017). The effluents of the industry generally contain inorganic pollutants that cause contamination of the aquatic environment and leads to deleterious effects such as chemical, physical, or biological threats. Subsequently, the removal of these contaminations is required by reducing their concentrations to acceptable levels (Bel et al. 2017). Various processes were developed for removing heavy metal ions: separation using membranes (Abu and Moussab 2004), coagulation (Charerntanyarak 1999), ion exchange, precipitation, adsorption, filtration, and electrodialysis (Anna and Hoek 2010). These methods all possess specific ad- and disadvantages. Serious disadvantages are incomplete metal removal, complex instrumentation, toxic byproducts, and high cost (Malkoc and Nuhoglu 2007). Among these methods, adsorption remains the best method for removing heavy metals especially if the adsorbent is efficient, cheap, and can be recycled (Lasheen et al. 2017). Activated carbon is a famous adsorbent used for the removal of both organic and inorganic pollutants but it is costly and sometimes difficult to be reused. More abundant adsorbents have attracted many researchers (Tor and Cengeloglu 2006) such as chitosan (Ngah et al. 2011), wheat shell (Basci et al. 2004), cacao shell (Meunier et al. 2003), natural zeolite (Erdem

Responsible editor: Tito Roberto Cadaval Jr

✉ Dler M. Salh Shwan
dler.salh@univsul.edu.iq

[1] College of Medical and Applied Sciences, Charmo University, Chamchamal 46023, Iraq

[2] Department of Chemistry, Clay and Environmental Chemistry Research Group, University of Sulaimani, Qlyasan Street, Sulaimani 46001, Iraq

[3] BGR Bundesansaltfür Geowissenschaften und Rohstoffe, Stilleweg 2, 30655 Hannover, Germany

et al. 2004), natural clay (Veli and Aly 2007), acid-activated clay (Aziz et al. 2011), and modified clay (Lin and Juang 2002) (Gopal and Sen 2008).

The adsorption capacity of a certain adsorber often depends on the pH. This can be either because of the pH-dependent speciation of the contaminant or because of pH-dependent surface charges of the adsorber. Dissolved Cd occurs as solvated cation below pH 7. No different species have to be distinguished. Above pH 7, however, Cd (as other heavy metals) tends to precipitate as hydroxide. The most interesting pH region to be studied is, therefore, below pH 7 (Çay et al. 2004) (Kumar and Bandyopadhyay 2006) (Sun et al. 2019).

Several researchers have developed methods for cadmium removal from aqueous solutions by using clay minerals like chitosan saturated montmorillonites (Hu et al. 2017), montmorillonites, kaolinite (Gupta and Bhattacharyya 2006), illite (Ozdes et al. 2011), and vermiculite (Abate and Masini 2005). The q_e values derived from the Langmuir isotherm models of these studies ranged from 7 to 50 mg/g.

The smectite clay minerals are belonging to phyllosilicates group which its structure is a stacking of negatively charged 2:1 layer, which is balanced by hydrated exchangeable cations fixed in interlayer positions like (Ca^{2+}, Mg^{2+}, and Na^{+}). Saponite is the most important trioctahedral smectites, which the trivalent cations replacing Si^{4+} cations in the tetrahedral sites processes the negative layer charge, and the vacancies in octahedral positions interpreted as the layer charge, and the basal spacing expansion of Saponite will approve the ability of cations accommodation in interlayer within the structural channels and at the external surface of lamellar particles (Pardo et al. 2018).

The clay minerals charge is regarded as the basis for the swelling and cation exchange properties. The charge results from permanent (structural) and variable (pH depending) charge. The cation exchange capacity (CEC) is a measure of both (Ismadji et al. 2015).

The aim of the present study was to characterize TC local clay for the first time and investigate the possible use of this clay as an efficient heavy metal ion adsorber for wastewater treatement. Due to the extreme toxicity of cadmium even at low concentrations and its wide usage, it was selected as a representative heavy metal ion in this study.

Materials and methods

Adsorbate

$Cd(NO_3)_2.4H_2O$ from Riedel-de HAEN AG was used to prepare a stock solution (500 mg/L) of Cd^{2+} from which the series of dilute solutions were prepared. The initial pH was adjusted with dilute HCl or NaOH, respectively. The Cd concentrations were measured using Inductively Coupled Plasma-Optical Emissions Spectroscopy (ICP-OES) (Perkin Elmer Optima 2100 DV) before and after adsorption tests. ICP-OES measurements required dilution of solutions.

Adsorbent characterization

The clay sample was taken in a depth of 50 cm in the Tagaran area near Sulaimani city-Kurdistan region of Iraq. The natural clay was dispersed in water and the < 5 μm fraction was separated by sedimentation. This fraction was termed TC (Tagaran clay) and used in the present study.

The chemical composition of TC was determined by XRF (PANalytica Axios, ALMELO, Netherlands). Lithium metaborate (Spectroflux, Flux No. 100A, Alfa Aesar) was mixed with the sample and melted into glass bead and analyzed by wavelength-dispersive XRF. The loss on ignition (LOI) was determined by heating 1000 mg of the sample material to 1030 ºC for 10 min.

A PANalytical X'Pert PRO MPD Θ-Θ diffractometer (Cu-K_α radiation, 40 kV, 30 mA) was used to record XRD patterns. The diffractometer was equipped with a variable divergence slit (20-mm irradiated length), primary and secondary soller, Scientific X'Celerator detector (active length 0.59º), and a sample changer (sample diameter 28 mm). The samples were investigated from 2º to 85º 2Θ with a step size of 0.0167º 2Θ and a measuring time of 10 s per step. For specimen preparation, the top loading technique was used. For the detailed clay mineralogical investigation, texture slides of the < 2 μm fraction was prepared. 15 mg per cm^2 clay was used to record an XRD scan. 1.5 mL of the suspension was vacuum filtered through the circular (diameter = 2.4 cm) ceramic tile to deposit the sample which were 3 mm thick. The specimen was ethylene glycol (EG) saturated with ethylene glycol vapor at 60 ºC overnight. The clay films were measured from 1º to 40º 2Θ (stepsize 0.03º 2Θ, 5 s per step) after cooling to room temperature, representing EG conditions. The interpretation of the XRD pattern, either powder or texture slides, were based on comparing the measured peak positions (either the 2-theta value or the *d* value) with suitable references, mostly from the PDF database.

The morphology and surface characteristics of the clay were investigated using scanning electron microscopy (SEM, FESEM: HITACHI S-4160).

Thermogravimetric analysis was performed using Diamond TG-DTA (SII) thermogravimetric analyzer from PerkinElmer using a 50 mL/min flow rate of N_2 inert gas from room temperature up to 900 ºC at a rate of 20 ºC/min.

Mid-infrared spectra were recorded for the sample pellet (1 mg sample/200 mg KBr) with a Thermo Nicolet Nexus FTIR spectrometer (MIR beam splitter: KBr, detector DTGS TEC). Measurements were conducted before and after drying of the pellets at 150 ºC in a vacuum oven for 24 h.

Autosorb-iQc-station 1 instrument from QuantaChrom was used for the investigation of N_2 adsorption–desorption isotherms. Measurements were performed at 77 K temperature. The sample was outgassed at 200 ºC 1000 h. Brunauer–Emmett–Teller (BET) theory was applied to N_2 adsorption data for the specific surface area (S_{BET}) investigation. The specific total pore volume (V_T) was calculated after the gas adsorption at a p/p_o of 0.99 that was converted to liquid volume using a value of 0.808 g cm^{-3} for the density of the adsorbed nitrogen.

The CEC of the Tagaran natural clay (TC) was measured using copper-trien method (Dohrmann et al. 2012). The Cu-trien complex solution (λ_{max} = 578 nm) was added to TC; the resulting slurry was shaken overnight for equilibration, and then centrifuged. The exchangable cations were measured from the difference between initial and remaining Cu-trien complex. The Cu-trien concentrations were measured by UV-Vis spectrophotometer at 578 nm.

Adsorption studies

For the batch adsorption experiments, 0.100 g of TC was added to 100-mL dark polyethylene bottles containing 50 mL of the Cd^{2+} solution with variable concentrations. The suspensions were shaken in a GFL waterbath shaker model 1086. After specific time intervals, the suspensions were centrifuged for 5 min at 5000 rpm. The Cd^{2+} concentrations in the supernatants were analyzed in the supernatant by ICP-OES. The amount of adsorbed (Cd^{2+}) ion, q_e (mg/g), was calculated using Eq. 1:

$$q_e = \frac{(C_o - C_e)V}{m} \tag{1}$$

where C_o and C_e represent the initial and equilibrium concentrations, respectively, V is the volume of the solution (L), and m is the mass of the adsorbent (g).

The effect of the contact time was investigated from 0 to 300 min at different temperatures. The influence of the initial pH of the Cd^{2+} solutions was studied at a range of 2.0 to 7.0. The pH values of the solutions were adjusted using dilute HCl or NaOH solutions with the aid of a pH meter. Adsorption isotherms were recorded by varying the initial Cd^{2+} concentration from 10 to 250 mg/L and measuring the extent of adsorption.

Error analysis

In addition to the error bars on the experimental data of the plots, the prediction of the model that best fit to the experimental data (isotherm and kinetic studies) were examined by three methods of error analysis for the non-linear curve fittings. First, the correlation index (coefficient of determination) (R^2) was calculated with the OriginPro software computer program (Eq. 2).

$$R^2 = 1 - \frac{\Sigma\left(q_{exp} - q_{fit}\right)^2}{\Sigma\left(q_{exp} - q_{mean}\right)^2} \tag{2}$$

where q_{fit} is the estimated value of q_{exp} for the model under investigation.

The second error function used was the sum of squared residuals (SSE) as given by Eq. 3.

$$SSE = \Sigma\left(q_{exp} - q_{fit}\right)^2 \tag{3}$$

The smaller values of SSE the better fit of the model under investigation.

The third error function was chi-squared (X^2) as given by Eq. 4.

$$X^2 = \Sigma\frac{\left(q_{exp} - q_{fit}\right)^2}{q_{fit}} \tag{4}$$

Similar to SSE, small values of X^2 represent a better fit of the model under study.

Application on real sample

Sulaimani industrial zone sewage was collected in a special container, digested by acid (5% nitric acid solution) in the laboratory, then separated from the solid particles by filtration.

The final solution was analyzed by ICP-OES technique with respect to dissolved ions particularly taking Cd into account. The pH of the solution was adjusted according to the Cd adsorption procedure and used as a real sample in the present work for adsorption application.

Results and discussion

Characterization of the adsorbent

From the XRD measurements, a 2:1 clay mineral (5.3º), quartz (26.6º), and calcite (29.2º) were identified. The d_{001} value of 14.9 Å (5.3º) may correspond to either vermiculite, chlorite, or smectite. Ethylene glycol (EG) vapor saturation (Fig. 1) proved limited expansion of the d_{001}-reflection from 14.9 to 16.8 Å. Commonly vermiculites do not expand to more than 16.1 Å with EG. The 2:1 clay mineral, therefore, is probably smectite (Mosser-Ruck et al. 2005). The d_{060} reflection showed no intensity at 1.49 Å but the significant intensity at 1.54 Å. The sample,

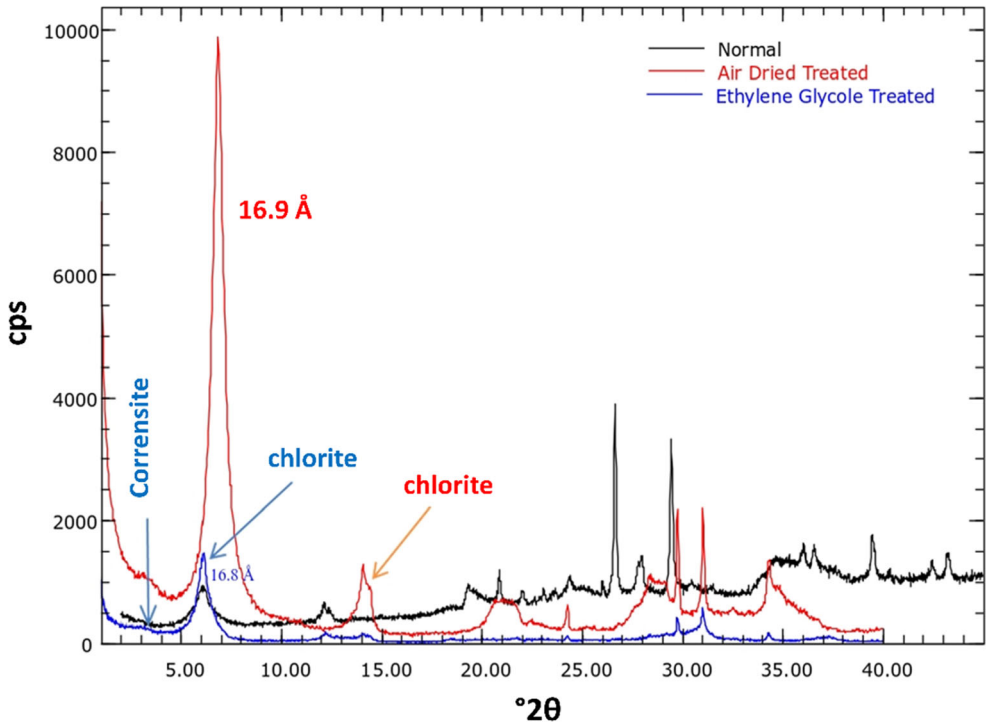

Fig. 1 XRD pattern of random (normal) powder, air dried, and ethylene glycol saturated oriented slides

therefore, is dominated by trioctahedral minerals with few dioctahedral domains or layers. The smectite is referred to as Saponite accordingly.

The small intensity (shoulder) which remained at 14.9 Å was attributed to chlorite. Two 7 Å peaks were observed. One was attributed to the d_{002} reflection of chlorite and the other could be explained by either kaolinite or serpentine. In the pattern of the oriented mount, weak and broad intensity was found at about 28 Å, which changed its position after EG treatment. This intensity was attributed to the presence of traces of corrensite.

FTIR spectra recorded from 400 to 4000 cm^{-1} before and after adsorption are shown in Fig. 2. It can be seen that the shape of the bands did not change upon adsorption but the stretching vibration bands after adsorption was slightly shifted compared with the bands after adsorption. The band at 3681 cm^{-1} in the FTIR spectrum (Fig. 2) could be assigned to either a serpentine mineral or trioctahedral smectite. No kaolinite was found (< 0.5 mass%) by IR. The second 7 Å XRD peak, therefore, was assigned to a serpentine mineral. The band at 3588 cm^{-1} results from OH-stretching of the serpentine mineral and the trioctahedral smectite. The bands at 3423and 1627 cm^{-1} were assigned to stretching and bending of water. The bands at 2925 and 2854 cm^{-1} point towards the presence of some organic material. The bands at 1434, 877, and 705 cm^{-1} proved the presence of calcite as dominating carbonate mineral. Quartz was identified based on the characteristic doublet at 780 and 800 cm^{-1}. The main band at about 1011 cm^{-1} represents SiO stretching modes of all silicates present in the sample (Arab et al. 2002) (Pazourková et al. 2014). The sample is dominated by a 2:1 clay mineral which based on almost full expandability and IR data was identified as trioctahedral smectite, in the following referred to as saponite.

The chemical composition of TC obtained with X-ray fluorescence was compared with the mineralogical composition (Table 1). Among those minerals identified by XRD and IR, saponite is that with most significant chemical variation. No information about the actual saponite composition was available. Because of the low amount of dioctahedral minerals and domains, the reference saponite composition published by webminerals.com was used (about 19% MgO, 11% Al_2O_3, 11% FeO, and 37.5% SiO_2). Based on the chemical data and the relative intensities of XRD peaks and IR bands, it is estimated that the sample consists of about 50% saponite (± 5%), 5–10% chlorite, 5% serpentine (± 2%), 10% calcite (± 2%), 20% quartz (± 3%), and 5% feldspar (± 3%). A few percents of the chlorite and the saponite occur as corrensite. The chemical and mineralogical composition of Saponite rich clays was discussed earlier (Muiambo et al. 2010) (Motokawa et al. 2014).

The SEM technique can be used to visualize individual particles of clays as well as the relative arrangement of particles to each other (microstructure). At least the shape and average size of the aggregates consisting of several primary particles can be observed in Fig. 3. The sample TC contains aggregates of various sizes apparently consisting of platy primary particles (Ding et al. 2017). The largest aggregates found had a diameter of 5–20 μm but most of the platy particles were

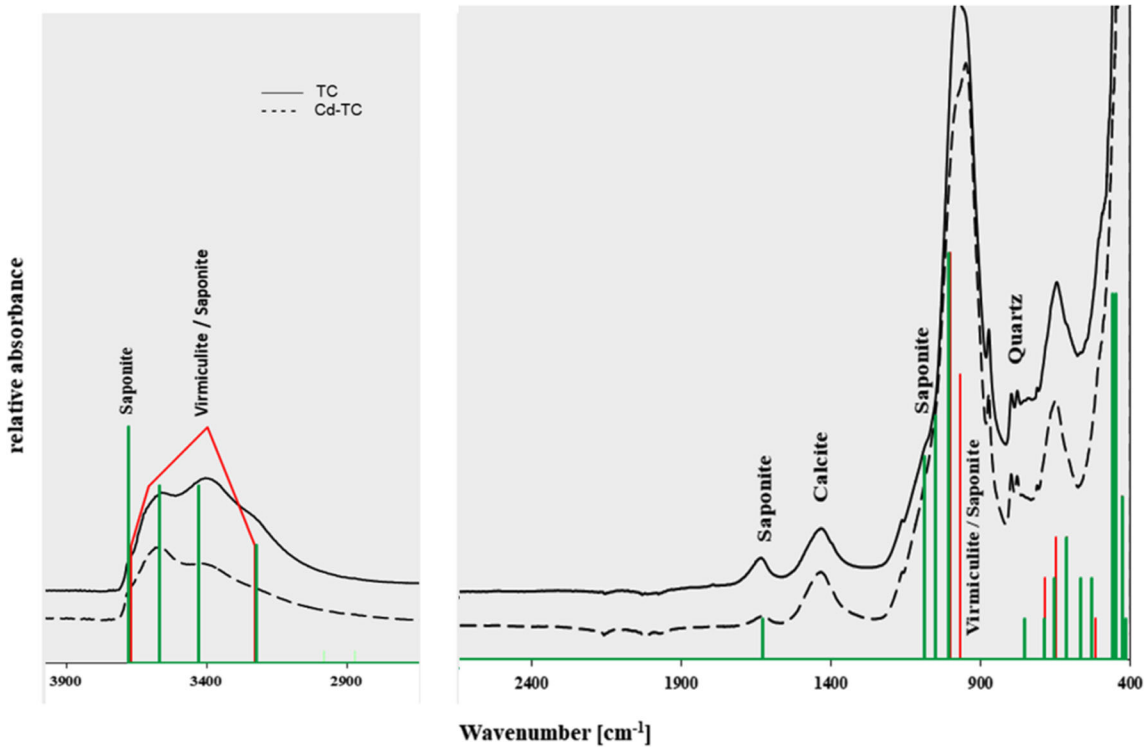

Fig. 2 FTIR spectra of TC before (TC) and after adsorption (Cd-TC) (dried at 150 ºC)

< 5 μm (Sutcu 2015). Individual particles that could be primary particles had a diameter of about 0.5 μm. The large particle on the lower left side of Fig. 3 showed either a network of cracks or a dense arrangement of primary particles with diameters between 0.1 and 0.2 μm. The particle size is typical of smectites.

The surface area and pore size distribution was calculated from N_2 adsorption isotherm (Fig. 4) at 77 K. The BET surface area was estimated as 51.4 m^2/g. The pore size distribution curve shows that most of the pores are less than 3 nm and a total pore volume of 0.0817 cm^3/g.

The TG/DTG plots (Fig. 5) show about 6% weight loss (dehydration) of adsorbed water molecules at 30 to 200 ºC. At the temperature range 200–500 ºC, where the interlayer water molecules are lost and the carbonate are also changes to CO_2 and CaO, no significant change has occurred due to the low carbonate content of the TC sample. A greater weight loss was observed between 500 and 800 ºC due to the dehydroxylation of the clay mineral and decomposition of carbonates.

The CEC obtained by Cu-trien method was 36 mmol/100 g.

Adsorption studies

Effect of contact time The effect of contact time on the adsorption of Cd^{2+} ions on the TC adsorbent was studied at different temperatures (Fig. 6). The amount of Cd^{2+} adsorbed rapidly increased at the early stage of the adsorption. After less than 1 h, the rate became slower and equilibrium was reached. The quick adsorption can possibly be explained by the high affinity of contaminant to the surface and the large excess of Cd^{2+}. In order to guarantee that equilibrium was attained, 100-min reaction time was set as a reference.

The maximum load of Cd^{2+} on TC varied from 11 to 13 mg Cd per g clay. This corresponds to about 11.4 mmol Cd^{2+} per 100 g clay or 22.8 meq/100 g. The measured CEC of the sample was about 36 meq/100 g (permanent and variable charge at pH about 7). The Cd load, therefore, was less than the CEC, theoretically leaving some remaining adsorption capacity. The Cd^{2+} excess, however, was significant and larger compared to most real cases. An even larger concentration of Cd^{2+} would have led to a larger portion of Cd^{2+} adsorbed to the clay but such high concentrations are not realistic; hence, it

Table 1 Chemical compositions of TC (values in mass%)

SiO_2%	TiO_2%	Al_2O_3%	Fe_2O_3%	MnO%	MgO%	CaO%	Na_2O%	K_2O%	SO_3%	LOI%	Total
43.4	0.5	9.9	8.6	0.1	14.6	6.8	0.7	0.8	0.1	14.2	99.7

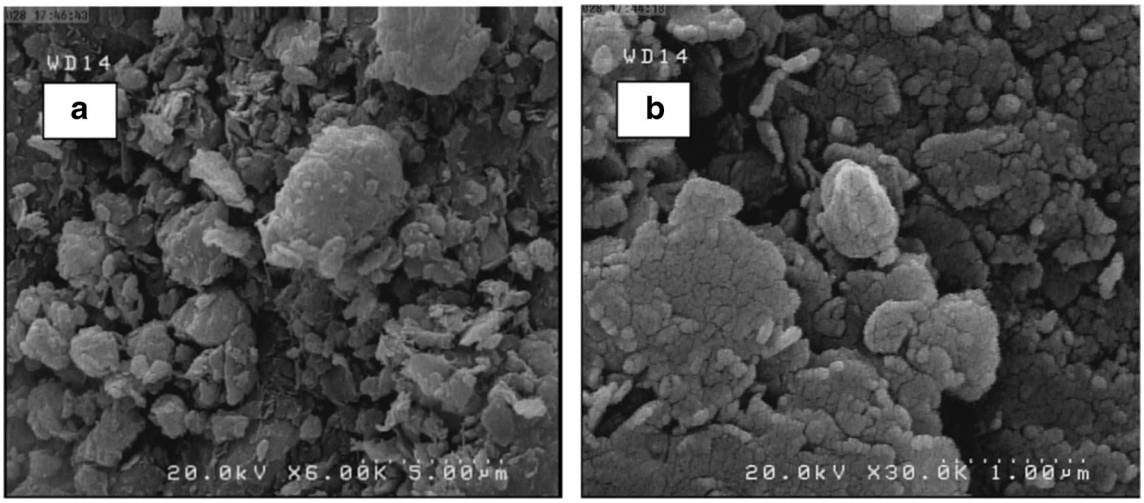

Fig. 3 SEM images of TC

can be concluded, that about 50% of the CEC may be relevant for Cd^{2+} removal.

The measured values correspond to the values reported in the literature, ranging from 7 to 50 mg/g (Abate and Masini 2005) (Gupta and Bhattacharyya 2006) (Ozdes et al. 2011) (Hu et al. 2017).

Effect of initial pH The most important factor that affects the removal of heavy metals by adsorption is the pH of the solution. This effect may be due to the hydrolysis reaction of the heavy metals and the formation of insoluble aqueous complexes as well as pH depending charges of the surfaces. Low adsorption capacities were observed at low pHs and they increased with increasing pH from 2 to 6, then reaching a constant value (Fig. 7). Similar results were obtained by Johnson (Johnson 1990). At pH higher than 7, precipitation of Cd species such as carbonates or hydroxides occurs (Chandra et al. 2006) (Rao and Kashifuddin 2016) (Xu et al. 2017) which affect the adsorption values.

Between pH 2.5 and 7, Cd^{2+} is known to be the dominant species. The lower adsorption capacity at low pH, therefore, must be related to pH depending changes at the clay surface. The pH effect on Cd^{2+} adsorption can be explained either by cation exchange competition of Cd^{2+} and H^{+} or by increasingly positive edge charges. The clay, however, is trioctahedral and hence, variable charge effects are supposed to be restricted to higher pH values.

Effect of adsorbent dose The adsorbent dose effect on the adsorption of Cd^{2+} was studied by using different doses in

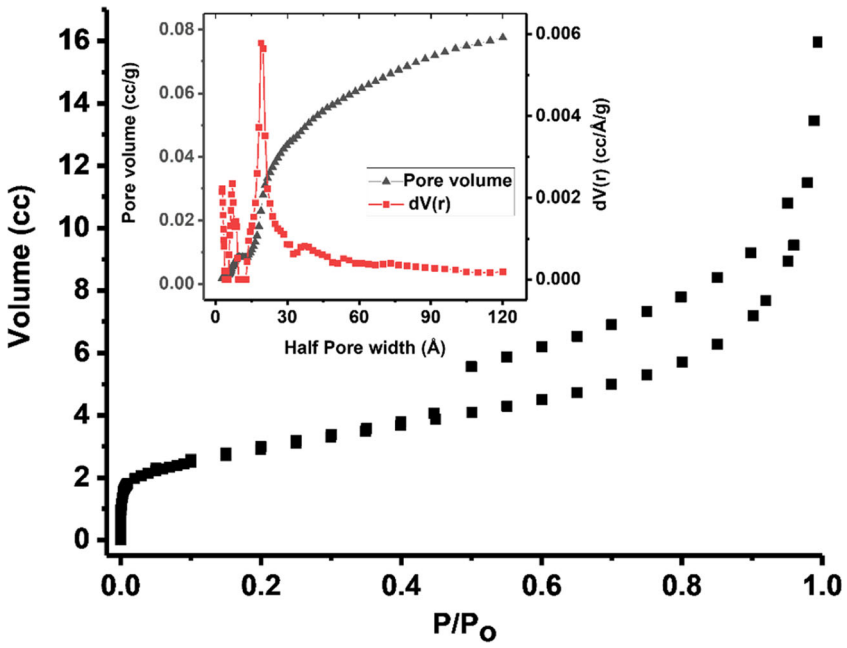

Fig. 4 N_2 adsorption isotherm with DFT fitting for the investigation of pore size distribution

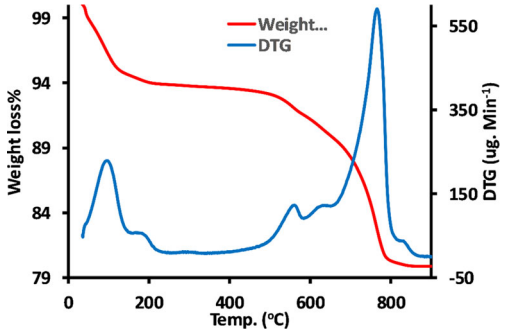

Fig. 5 TG/DTG plots of TC (heating rate 20 ºC/min, 50 mL/min N_2 gas flow)

the range from 0.02 to 0.25 g at fixed conditions of pH = 6.0 and 100 mg/L initial Cd^{2+} concentration. As the dose of adsorbent increases from 0.02 to 0.25 g, the adsorbed amount of Cd^{2+} per unit weight of TC (q_e) decreases (Fig. 8) because the adsorbed amount of Cd^{2+} (mg) is divided by the larger amount of adsorbent (g) in the nominator of Eq. 1 and this was expected because all experiments were conducted below saturation. Meanwhile, the removal % increases steadily with increasing the adsorbent dose.

Effect of initial Cd^{2+} concentration An increasing concentration gradient acts as increasing driving force towards adsorption and hence, leads to increasing equilibrium adsorption until saturation achieved. The initial concentration of Cd^{2+} was studied in the range between10 and 250 mg/L. The adsorption was carried out at a fixed pH of 6.0 and 0.1 g TC at four different temperatures 20, 30, 40, and 50 ºC (Fig. 9). The values of q_e increased with increasing initial Cd^{2+} concentrations under the studied range of concentrations. A slight decrease in q_e is noticed which may result from increased desorption. Meanwhile, removal % has decreased with increasing C_o.

Adsorption isotherms A good description of the distribution of the adsorbate between solution and adsorbent at equilibrium conditions is important for the determination of the mechanism of Cd^{2+} adsorption. The surface properties and the

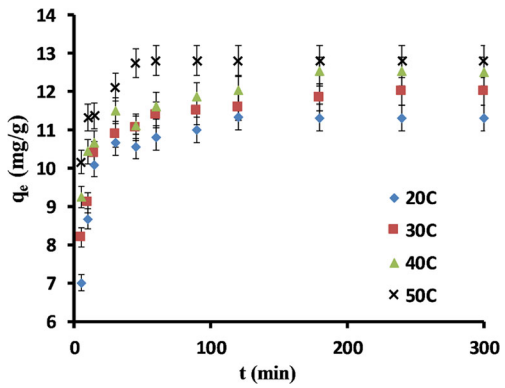

Fig. 6 Effect of contact time on the adsorption of Cd^{2+} (C_o = 100 mg/L) on TC at different temperatures

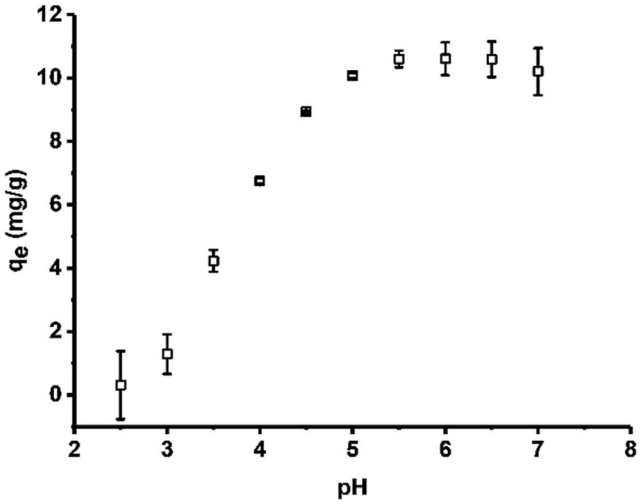

Fig. 7 Effect of initial pH on the adsorption of Cd^{2+} (C_o = 100 mg/L, 0.1 g TC) on TC at room temperature

affinity of the adsorbent towards Cd^{2+} can be obtained from the constants of the adsorption isotherms(Malkoc and Nuhoglu 2007). Langmuir, Freundlich, Temkin, and Redlich-Peterson isotherms were applied to the experimental data of this study using non-linear regression analysis.

Langmuir isotherm The Langmuir isotherm model predicts the formation of monolayer adsorption of the adsorbate on the adsorbent surface (Eq. 5). (Langmuir 1918).

$$q_e = \frac{q_m K_L C_e}{1 + K_L C_e} \tag{5}$$

where q_e and C_e are the amount adsorbed and the adsorbate concentration in solution at equilibrium, respectively. K_L is the Langmuir constant and q_m is the maximum amount of the monolayer adsorbed on the adsorbent, and C_o is the initial adsorbate concentration. The values of K_L and q_m were

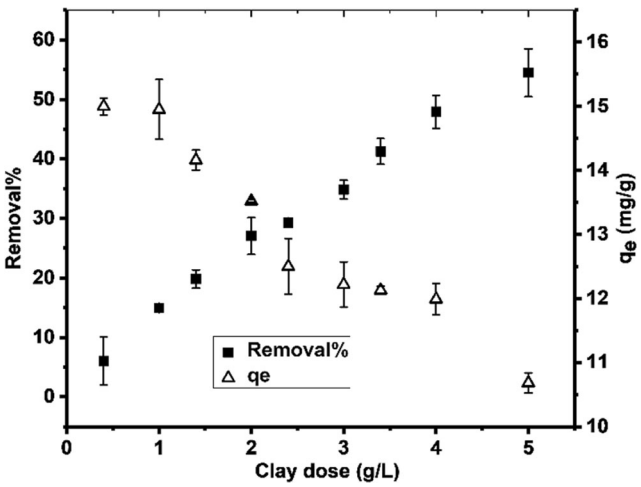

Fig. 8 Effect of adsorbent dosage on Cd^{2+} adsorption (C_o = 100 mg/L, initial pH = 6.0, T = 293 K)

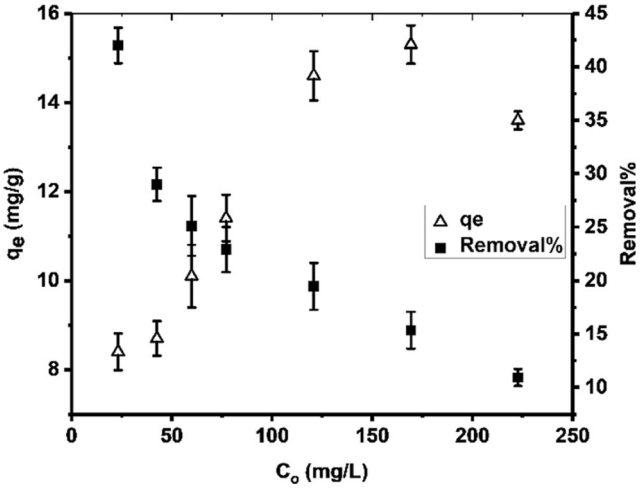

Fig. 9 Effect of initial concentration of Cd^{2+} on q_e and removal% by TC (0.1 g TC, initial pH = 6.0, T = 293 K)

computed from the non-linear regression analysis at different temperatures (Fig. 10) (Table 2).

Freundlich isotherm The Freundlich isotherm model describes the adsorption of an adsorbate on a heterogeneous adsorbent surface considering multilayer adsorption. Equation 6 represents the linearized Freundlich isotherm (Appel 1973):

$$q_e = K_f C_e^{1/n} \tag{6}$$

where K_F and n are Freundlich constants representing adsorption capacity and intensity respectively. Adsorption isotherm constants. For heterogeneous adsorption, 1/n is approaching zero, while for chemisorption the slope is in between 0 and 1, and a value greater thn 1 indicates cooperative adsorption (Asgari et al. 2014). The Freundlich isotherm was applied to the experimental data (Fig. 10) from which the isotherm constants were estimated (Table 2).

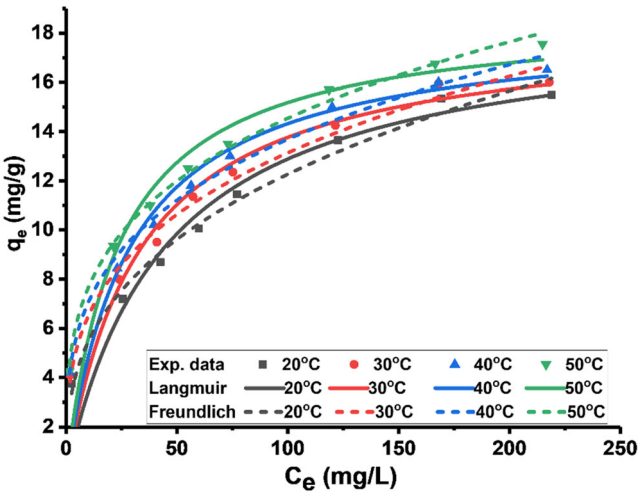

Fig. 10 Langmuir and Freundlich isotherm models for the adsorption of Cd^{2+} on TC at different temperatures (0.1 g TC, initial pH = 6.0)

Temkin isotherm According to this isotherm, the heat of adsorption decreases linearly with coverage due to adsorbent–adsorbate interactions with a uniform distribution of the adsorbate. The Temkin isotherm is represented by Eq. 7:

$$q_e = B\ln A + B\ln C_e \tag{7}$$

where $B = RT/b$ is related to the heat of adsorption, R is the universal gas constant (J mol^{-1} K^{-1}), T is the temperature K, and b is the variation of adsorption energy (J/mol). The Temkin isotherm model was applied to evaluate the adsorbent–adsorbate interactions (Fig. 11) (Table 2).

Redlich–Peterson isotherm Redlich–Peterson (R–P) isotherm is a three-parameter isotherm that rectifies the inaccuracy of the two-parameter isotherms (Langmuir and Freundlich) and it is a combination between them. The isotherm is given by Eq. 8.

$$q_e = \frac{K_{RP} C_e}{1 + a_{RP} C_e^{\beta}} \tag{8}$$

where K_{RP} (l/mg) and a_{RP} (l/mg) are the R–P constants and β is an exponent that varies from 0 to 1. From the non-linear regression of Redlich–Peterson isotherms (Fig. 11), the isotherm parameters were estimated (Table 2).

The Redlich parameter (β) was found to be less than 1 and the studied error functions of the isotherms reveal that the Freundlich model approximation better fits the experimental data than Langmuir model (Areco and Afonso 2010).

It is not easy to compare the adsorption of different heavy metal ions on natural clay from different sources. Many factors may affect the adsorption capacity during the adsorption such as pH, clay source, and clay particle size. Adsorption of some heavy metal ions on natural clay are explored in Table 3.

Kinetic studies

The study of adsorption kinetic is important to explore the adsorbate–adsorbent interaction. Three most common kinetic models were applied to the experimental data: Lagergren pseudo-first order (Baek et al. 2010), Ho's pseudo-second order (Ho 2006), and Weber's intra-particle diffusion (Alkan et al. 2008).

The Lagergren pseudo-first-order kinetics is given by Eq. 9 (Fig. 12a):

$$q_t = q_e\left(1 - e^{-k_1 t}\right) \tag{9}$$

where k_1 is the pseudo-first-order rate constant (min^{-1}) of adsorption, q_e and q_t are the amounts of the metal ion (mg/g) adsorbed at equilibrium and at time t.

Table 2 Adsorption isotherm parameters of Cd^{2+} on TC at different temperatures

Isotherm models	Isotherm parameters	T (K)			
		293	303	313	323
Langmuir	q_m (mg/g)	18.21	18.32	18.35	18.78
	K_L (L/mg)	0.0223	0.0302	0.0356	0.0422
	r^2	0.926	0.907	0.910	0.913
	SSE	8.8	11.1	11.1	11.7
	X^2	1.5	1.9	1.8	1.9
Freundlich	N	2.8	3.3	3.5	3.6
	K_F	2.43	3.21	3.63	4.02
	r^2	0.987	0.987	0.989	0.996
	SSE	1.6	1.6	1.3	0.6
	X^2	0.3	0.3	0.2	0.1
Temkin	B (J/mol)	2.77	2.61	2.61	2.72
	K_T	0.91	1.63	2.01	2.20
	r^2	0.910	0.925	0.942	0.962
	SSE	10.7	8.9	7.1	5.2
	X^2	1.8	1.5	1.2	0.9
Redlich-Peterson	K_{RP} (1/mg)	42.6	38.6	31.5	21.3
	α_{rp}	17.2	11.7	8.3	4.9
	B	0.65	0.70	0.72	0.74
	R^2	0.986	0.986	0.989	0.997
	SSE	1.6	1.6	1.3	0.4
	X^2	0.32	0.33	0.27	0.08

A second-order dependency of the adsorption rate on the adsorption sites is given by Eq. 10. Integration of Eq. 10 with applied limits of q_t between 0 and q_t when t is passed from 0 to t results in Eq. 11.

$$\frac{dq}{dt} = k_2(q_e - q_t)^2 \tag{10}$$

$$q_t = \frac{k_2 q_e^2 t}{1 + k_2 q_e^2 t} \tag{11}$$

where k_2 is the pseudo-second-order rate constant (g/mg min). Pseudo-second-order kinetic plots for the adsorption of Cd^{2+} on TC was studied at different temperatures (Fig. 12a) and the corresponding kinetic parameters were estimated from non-linear regression fittings (Table 4). The studied error analysis functions revealed better fitting of the pseudo-second-order kinetics to the experimental data. The correlation coefficients of pseudo-second-order kinetics are closer to unity than those of pseudo-first-order kinetics, and Δq, *SSE*, and X^2 values for the pseudo-second-order kinetic model are much smaller than those for the pseudo-first-order model.

The diffusion-controlled adsorption system was investigated by using the intra-particle diffusion model, described by Eq. 12.

$$q_t = k_i . t^{0.5} + C \tag{12}$$

where k_i is the intra-particle diffusion rate constant (mg/g $min^{1/2}$) and C is related to the boundary layer thickness, i.e., the larger the intercept, the greater is the boundary effect. The plots of q_t vs $t^{0.5}$ at various temperatures (Fig. 12b) show multi-linear curves and none of these linear parts is passing through the origin. This suggests that intra-particle diffusion is not the rate determining step and not the only mechanism governing the rate of the adsorption. From the plots, first,

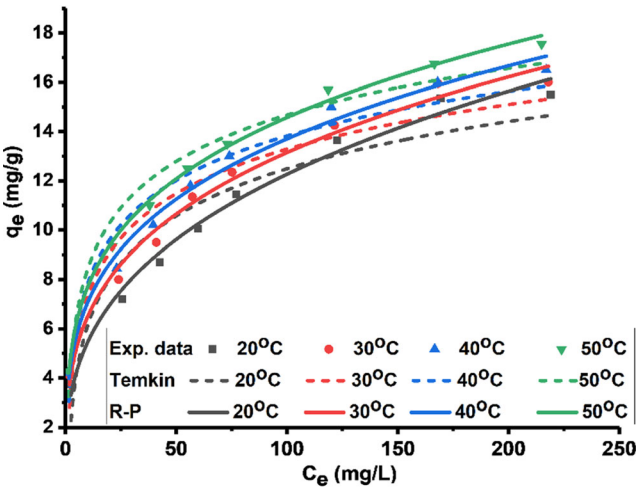

Fig. 11 Temkin and Redlich–Peterson isotherms for the adsorption of Cd^{2+} on TC at different temperatures (0.1 g TC, initial pH = 6.0)

Table 3 Adsorption capacities different heavy metal ions on natural clay

Adsorbent	Heavy metal ion	Adsorption capacity	Reference
Natural clay	Cu^{2+}	44.84	(Jiang et al. 2010)
Natural sepiolite	Cr^{2+}	37.00	(Marjanović et al. 2013)
Kaolinite	Pb^{2+}	11.5	(Sen Gupta and Bhattacharyya 2008)
Natural clay	Mn^{2+}	11.36	(Ondo 2010)
Natural clay	Hg^{2+}	9.7	(Eloussaief et al. 2013)

relatively fast surface sorption of Cd^{2+} ion on the external surface to saturation, then followed by a slower step of intra-particle diffusion which was apparently the rate limiting (Alkan et al. 2008). Finally, the third region may be attributed to the final equilibrium stage. The results indicate that the interlayer surfaces are readily accessible sites for exchange with the incoming cadmium. The dominating adsorption mechanism, therefore, is cation exchange at permanent charged surface sites. In addition, adsorption at edge sites may also be important but that could not be proved.

The effect of temperature on the equilibrium adsorption capacity and the rate of adsorption was illustrated using Arrhenius (Eq. 13) and Eyring (Eq. 14) equations.

$$\ln k_2 = \ln A - \frac{E_a}{RT} \tag{13}$$

$$\ln \frac{k_2 h}{k_B T} = \ln \frac{\Delta S^*}{R} - \frac{\Delta H^*}{RT} \tag{14}$$

where E_a is the activation energy (J/mol), k_2 is the pseudo-second-order rate constant for adsorption (g/mol s), A is the temperature-independent Arrhenius constant (g/mol s), R is the gas constant (8.314 J/K mol), ΔS^* is the entropy of activation (J/mol), and ΔH^* is the enthalpy of activation (kJ/mol). Arrhenius and Eyring's plots are shown in Fig. 13 and the activation parameters are listed in Table 4. Low activation energies ($E_a < 40$ kJ/mol) indicate a physical adsorption mechanism, while higher E_a (40–800 kJ/mol) points to a chemically controlled mechanism. The E_a in this study is 16.8 kJ/mol which suggests a physisorption mechanism.

The negative value of ΔS^* indicates the association of Cd^{2+} ions in the excited state before the release of the leaving ion or group.

Thermodynamic studies

Gibb's free energy change (ΔG^o) was determined at different temperatures by Eq. (15) (Frantz et al. 2017).

$$\Delta G^o = -RT \ln(\rho_W K_D) \tag{15}$$

Van't Hoff's plot was used to estimate the enthalpy change (ΔH^o) and entropy change (ΔS^o) (Table 5) according to Eq. 16:

$$\ln(\rho_W K_D) = \frac{\Delta S^o}{R} - \frac{\Delta H^o}{RT} \tag{16}$$

The values of ΔG^o at all temperatures were negative and decreasing with increasing temperature which indicates the spontaneous nature of the adsorption of Cd^{2+} on TC and better adsorption occurs at higher temperatures (Ahmed et al. 2017).

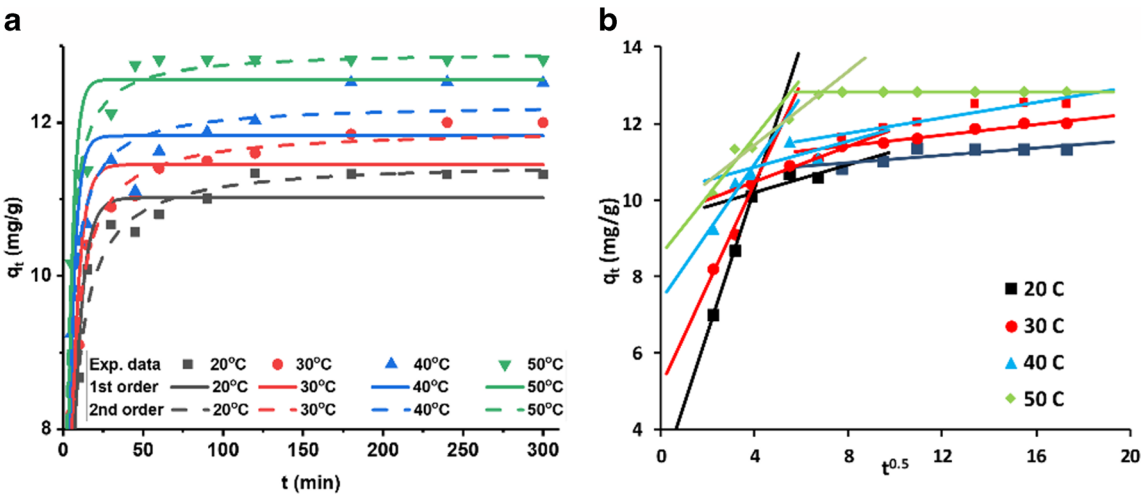

Fig. 12 Non-linear regression plots of pseudo-first-order and pseudo-second-order kinetics of the adsorption of Cd^{2+} on TC (**a**) and intra-particle diffusion plots for the adsorption of Cd^{2+}on TC (**b**) (C_o = 100 mg/L, pH = 6.0)

Table 4 Kinetic model parameters for the adsorption of Cd^{2+} on TC

Kinetic models	Parameters	T (K)			
		293	303	313	323
	$q_{e(exp)}$ (mg/g)	11.5	11.83	12.53	12.82
Pseudo first-order	k_1 (min^{-1})	0.178	0.205	0.269	0.298
	$q_{e(calc.)}$ (mg/g)	11.0	11.5	5.26 11.8	1.67 12.6
	Δq%	4.2	3.2	5.6	2.0
	R^2	0.990	0.945	0.870	0.717
			0.976	0.972	0.969
	SSE	1.2	3	0.4	2.2
	X^2	0.1	0.3	0.4	0.2
Pseudo second-order	k_2 (g/mg min)	0.0289	0.0068	0.0226	0.0558
			0.0333	0.0455	0.0531
	$q_{e(calc.)}$	11.50	11.90	12.61	12.95
			11.92	12.24	12.93
	Δq%	0.0	- 0.8	2.3	- 0.9
	R^2	0.996	0.999 0.996	0.999 0.992	0.999 0.998
	SSE	0.46	0.45	1.09	0.34
	X^2	0.05	0.05	0.11	0.03
Intra-particle diffusion	k_{p1} (mg/g $min^{0.5}$)		1.621	0.888	0.768
	k_{p2} (mg/g $min^{0.5}$)		0.637	0.039	0.315
	k_{p3} (mg/g $min^{0.5}$)		0.305	0.161	0
Arrhenius equation	E_a (kJ/mol)	16.80			
Eyring equation	ΔH* (kJ/mol)	14.2			
	ΔS* (J/mol)	- 225.9			

The positive value of ΔH^o indicates the endothermic nature of adsorption and the positive value of ΔS^o reflects the increased randomness at the solid/solution interface during the adsorption process.

A predominant cation exchange mechanism is suggested for the uptake of Cd^{2+} ions in the early stages of the adsorption. At low pHs, H^+ ions compete with Cd^{2+} ions for the permanent charges and lower adsorption capacity was recorded. The uptake of Cd^{2+} becomes slower after that and the mechanism may be inner-sphere surface complex formation of the cations at the clay edges that migrated from basal planes exchange sites (Dal Bosco et al. 2006).

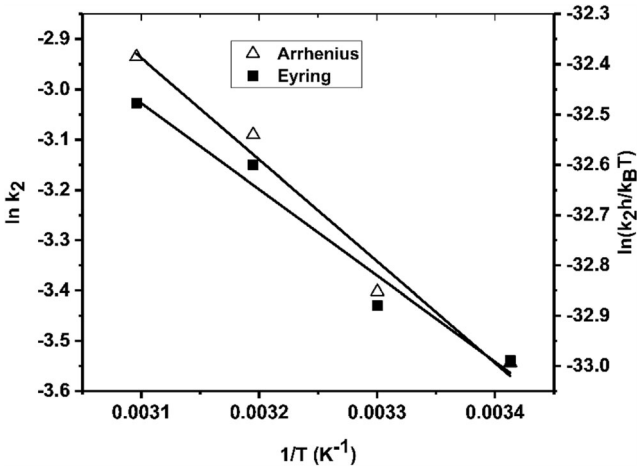

Fig. 13 Arrhenius and Eyring plots for the adsorption of Cd^{2+} on TC

Applications on real samples

Sulaimani industrial zone sewage was taken as the real sample which contains noticeable heavy metals (9.4, 26.0, 229.9, 260.0) μg/L for (Cd, Cr, Fe, Zn) respectively. The pH was adjusted to 6–6.2 with dilute HCl and/or NaOH solution and adsorption experiments were

Table 5 Thermodynamic parameters for Cd^{2+}adsorption on TC

Temp. (K)	Thermodynamic parameters		
	ΔG° (kJ/mol)	ΔH° (kJ/mol)	ΔS° (J/mol K)
293	- 9.72	1.46	38.12
303	- 10.08		
313	- 10.45		
323	- 10.87		

conducted using the TC clay described in the present study. The resulting concentrations after adsorption were (0.01., 25.43, 229.80, 172.90) μg/L for (Cd, Cr, Fe, Zn) respectively. This result shows that the Cd ion was completely removed (adsorbed) by TC. Other elements as Cr and Fe ions were not reduced, probably because their maximum adsorption occurs at pH = (2 and ≤ 4) (Malkoc and Nuhoglu 2007) (Bhattacharyya and Gupta 2008). Zn, in contrast, was partially removed from the solution which could have been expected because Zn ions have a good adsorption potential at pH = 6.5 (Purna Chandra Rao et al. 2006). Zn and Cd, hence, were competing for the adsorption sites resulting in 100% removal of Cd and about 30% removal of Zn.

Conclusions

In the present work, the natural clay of Tagaran from Sulaimani/Iraq was characterized by XRF, XRD, FTIR, and SEM. Its major constituent is saponite. After physical cleaning and fractionation, the natural clay was studied for its efficiency for the adsorption of Cd^{2+}, a very toxic heavy metal ion. The initial pH of the solution showed a significant effect on the adsorption and best efficiencies were obtained at moderate and higher pHs.

Both Langmuir and Freundlich isotherm models fit well to the adsorption data. The kinetic data were better explained by pseudo-second-order kinetics and the rate-determining step is governed by more than one mechanism as confirmed by the intra-particle diffusion kinetics. The activation energy (16.8 kJ/mol) for the adsorption of Cd^{2+} on TC falls in the range of a physisorption process. The spontaneity of the adsorption was confirmed by the negative values of ΔG^{o} at the studied temperatures and the affinity of the adsorbent to the adsorbate was confirmed by the positive values of ΔS^{o}. The natural clay from Tagaran is a local candidate adsorber material for the removal of Cd from industrial wastewater. The local natural clay (TC) was successfully applied for the removal of cadmium from Sulaimani industrial zone sewage despite the presence of other heavy metals. Further studies dealing with the application of recycling, and mechanical stability of the adsorber, however, have to be performed.

Acknowledgments We gratefully acknowledge Federal Institute for Geosciences and Natural Resources (BGR), for the support and their assistance and all who contributed to conduction of this study.

Compliance with ethical standards

Conflict of interest The authors declare that they have no conflict of interest.

References

Abate G, Masini JC (2005) Influence of pH, ionic strength and humic acid on adsorption of Cd(II) and Pb(II) onto vermiculite. Colloids Surf A Physicochem Eng Asp 262:33–39

Abu, H. and Moussab, H. (2004) Removal of heavy metals from wastewater by membrane processes : a comparative study. **164**, 105–110

Ahmed, H.R., Raheem, S.J., and Aziz, B.K. (2017) Removal of Leishman stain from aqueous solutions using natural clay of Qulapalk area of Kurdistan region of Iraq. *Karbala International Journal of Modern Science*, **3**, 165–175. Elsevier ltd.

Alkan M, Doğan M, Turhan Y, Demirbaş Ö, Turan P (2008) Adsorption kinetics and mechanism of maxilon blue 5G dye on sepiolite from aqueous solutions. Chem Eng J 139:213–223

Anna J, Hoek EMV (2010) Removing cadmium ions from water via nanoparticle-enhanced ultrafiltration. Environ Sci Technol 44: 2570–2576

Appel J (1973) Freundlich's adsorption isotherm. Surf Sci 39:237–244

Arab M, Bougeard D, Smirnov KS (2002) Experimental and computer simulation study of the vibrational spectra of vermiculite. Phys Chem Chem Phys 4:1957–1963

Areco MM, Afonso S (2010) Colloids and surfacesB: biointerfaces copper, zinc, cadmium and lead biosorption by Gymnogongrus torulosus. Thermodynamics and Kinetics Studies 81:620–628

Asgari M, Anisi H, Mohammadi H, Sadighi S (2014) Designing a commercial scale pressure swing adsorber for hydrogen purification. Petroleum and Coal 56:552–561

Aziz BK, Abdullah MA, Jubrael KJ (2011) Acid activation and bleaching capacity of some clays for decolourizing used oils. Asian J Chem

Baek MH, Ijagbemi CO, O SJ, Kim DS (2010) Removal of malachite green from aqueous solution using degreased coffee bean. J Hazard Mater 176:820–828

Basci, N., Kocadagistan, E., and Kocadagistan, B. (2004) Biosorption of copper(II) from aqueous solutions by wheat shell. **164**, 135–140

Bel, H., Sdiri, A., Ltaief, W., Da, P., Ben, M., and Galves, M.E. (2017) Comptes Rendus Chimie Efficient removal of cadmium and 2-chlorophenol in aqueous systems by natural clay: adsorption and photo-Fenton degradation processes

Bhattacharyya KG, Gupta SS (2008) Adsorption of a few heavy metals on natural and modified kaolinite and montmorillonite: a review. Adv Colloid Interf Sci 140:114–131

Çay S, Uyanik A, Özaşik A (2004) Single and binary component adsorption of copper(II) andcadmium(II) from aqueous solutions using tea-industry waste. Sep Purif Technol 38:273–280

Chamsaz M, Atarodi A, Eftekhari M, Asadpour S, Adibi M (2013) Vortex-assisted ionic liquid microextraction coupled to flame atomic absorption spectrometry for determination of trace levels of cadmium in real samples. *J Adv Res* 4:35–41 Cairo University

Chandra, G.P., Satyaveni, S., Ramesh, A., Seshaiah, K., Murthy, K.S.N., and Choudary, N. V. (2006) Sorption of cadmium and zinc from aqueous solutions by zeolite 4A , zeolite 13X and bentonite. **81**, 265–272

Charerntanyarak, L. (1999) Heavy metals removal by chemical coagulation and. *Water Science and Technology*, **39**, 135–138. International association on water quality

Dal Bosco SM, Jimenez RS, Vignado C, Fontana J, Geraldo B, Figueiredo FCA, Mandelli D, Carvalho WA (2006) Removal of Mn(II) and Cd(II) from wastewaters by natural and modified clays. Adsorption 12:133–146

Ding, F., Gao, M., Wang, J., Shen, T., and Zang, W. (2017) Tuning wettability by controlling the layer charge and structure of organo-vermiculites. Journal of Industrial and Engineering Chemistry. The Korean Society of Industrial and Engineering Chemistry

Dohrmann R, Genske D, Karnland O, Kaufhold S, Kiviranta L, Olsson S, Plötze M, Sandén T, Sellin P, Svensson D, Valter M (2012)

Interlaboratory CEC and exchangeable cation study of bentonite buffer materials: I. Cu(II)-triethylenetetramine method. Clay Clay Miner 60:162–175

Eloussaief M, Sdiri A, Benzina M (2013) Modelling the adsorption of mercury onto natural and aluminium pillared clays. Environ Sci Pollut Res 20:469–479

Erdem, E., Karapinar, N., and Donat, R. (2004) The removal of heavy metal cations by natural zeolites. **280**, 309–314

Frantz TS, Silveira N, Quadro MS, Andreazza R, Barcelos AA, Cadaval TRS, Pinto LAA (2017) Cu(II) adsorption from copper mine water by chitosan films and the matrix effects. *Environ Sci Pollut Res* **24**: 5908–5917

Gopal, K. and Sen, S. (2008) Adsorption of a few heavy metals on natural and modified kaolinite and montmorillonite: a review. **140**, 114–131

Gupta SS, Bhattacharyya KG (2006) Removal of Cd(II) from aqueous solution by kaolinite, montmorillonite and their poly(oxo zirconium) and tetrabutylammonium derivatives. *J Hazard Mater* 128: 247–257

Ho YS (2006) Review of second-order models for adsorption systems. J Hazard Mater 136:681–689

Sen Gupta S, Bhattacharyya KG (2008) Immobilization of Pb(II), Cd(II) and Ni(II) ions on kaolinite and montmorillonite surfaces from aqueous medium. J Environ Manag 87:46–58

Hu C, Zhu P, Cai M, Hu H, Fu Q (2017) Comparative adsorption of Pb(II), Cu(II) and Cd(II) on chitosan saturated montmorillonite: kinetic, thermodynamic and equilibrium studies. *Appl Clay Sci* **143**: 320–326 Elsevier

Hwang, D.F. and Wang, L.C. (2001) Effect of taurine on toxicity of cadmium in rats. **167**, 173–180

Ismadji, S., Soetaredjo, F.E., and Ayucitra, A. (2015) Clay materials for environmental remediation. **P. in.**:

Jiang MQ, Jin XY, Lu XQ, Chen ZL (2010) Adsorption of Pb(II), Cd(II), Ni(II) and Cu(II) onto natural kaolinite clay. *Desalination* **252**:33–39 Elsevier BV

Johnson BB (1990) Effect of pH, temperature, and concentration on the adsorption of cadmium on goethite. Environ Sci Technol 24:112–118

Kumar U, Bandyopadhyay M (2006) Sorption of cadmium from aqueous solution using pretreated rice husk. Bioresour Technol 97:104–109

Langmuir I (1918) The adsorption of gases on plane surfaces of glass, mica and platinum. J Am Chem Soc 40:1361–1403

Lasheen, M.R., El-sherif, I.Y., and El-wakeel, S.T. (2017) Heavy metals removal from aqueous solution using magnetite Dowex 50WX4 resin nanocomposite. **8**, 503–511

Lin, S. and Juang, R. (2002) Heavy metal removal from water by sorption using surfactant-modified montmorillonite. **92**, 315–326

Malkoc E, Nuhoglu Y (2007) Determination of kinetic and equilibrium parameters of the batch adsorption of Cr(VI) onto waste acorn of Quercus ithaburensis. Chem Eng Process Process Intensif 46:1020–1029

Marjanović V, Lazarević S, Janković-Častvan I, Jokić B, Janaćković D, Petrović R (2013) Adsorption of chromium(VI) from aqueous solutions onto amine-functionalized natural and acid-activated sepiolites. Appl Clay Sci 80–81:202–210

Meunier, N., Laroulandie, J., Blais, J.F., and Tyagi, R.D. (2003) Cocoa shells for heavy metal removal from acidic solutions. **90**, 255–263

Mosser-Ruck R, Devineau K, Charpentier D, Cathelineau M (2005) Effects of ethylene glycol saturation protocols on XRD patterns: a critical review and discussion. Clay Clay Miner 53:631–638

Motokawa R, Endo H, Yokoyama S, Ogawa H, Kobayashi T, Suzuki S, Yaita T (2014) Mesoscopic structures of vermiculite and weathered biotite clays in suspension with and without cesium ions. Langmuir 30:15127–15134

Muiambo HF, Focke WW, Atanasova M, van der Westhuizen I, Tiedt LR (2010) Thermal properties of sodium-exchanged palabora vermiculite. *Appl Clay Sci* **50**:51–57 Elsevier B.V

Ngah WSW, Teong LC, Hanafiah MAKM (2011) Adsorption of dyes and heavy metal ions by chitosan composites: a review. *Carbohydr Polym* **83**:1446–1456 Elsevier ltd.

Ondo JA (2010) Evaluation of the absorption capacity of the natural clay from Bikougou (Gabon) to remove Mn (II) from aqueous solution. Int J Eng Sci Technol 2:5001–5016

Ozdes D, Duran C, Senturk HB (2011) Adsorptive removal of Cd(II) and Pb(II) ions from aqueous solutions by using Turkish illitic clay. *J Environ Manag* **92**:3082–3090 Elsevier ltd.

Pardo L, Cecilia J, López-Moreno C, Hernández V, Pozo M, Bentabol M, Franco F (2018) Influence of the structure and experimental surfaces modifications of 2:1 clay minerals on the adsorption properties of methylene blue. Minerals 8:359

Pazourková, L., Martynková, G.S., Hundáková, M., and Barošová, H. (2014) M Ontmorillonite and vermiculite modified by N-vinylcaprolactam and poly (N-vinylcaprolactam) preparation and characterization. 1–6

Purna Chandra Rao G, Satyaveni S, Ramesh A, Seshaiah K, Murthy KSN, Choudary NV (2006) Sorption of cadmium and zinc from aqueous solutions by zeolite 4A, zeolite 13X and bentonite. J Environ Manag 81:265–272

Rao RAK, Kashifuddin M (2016) Adsorption studies of Cd(II) on ball clay: comparison with other natural clays. *Arab J Chem* **9**:S1233–S1241 King Saud University

Roushani, M., Saedi, Z., and Baghelani, Y.M. (2017) Environmental nanotechnology, monitoring & management removal of cadmium ions from aqueous solutions using TMU-16-NH 2 metal organic framework. *Environmental Nanotechnology, Monitoring & Management*, **7**, 89–96. Environmental Nanotechnology, Monitoring & Management

Sun Q, Liu C, Cui P, Fan T, Zhu M, Alves ME, Siebecker MG, Sparks DL, Wu T, Li W, Zhou D, Wang Y (2019) Formation of Cd precipitates on Γ-Al 2 O 3: implications for Cd sequestration in the environment. *Environ Int* **126**:234–241 Elsevier

Sutcu M (2015) Influence of expanded vermiculite on physical properties and thermal conductivity of clay bricks. *Ceram Int* **41**:2819–2827 Elsevier

Tor A, Cengeloglu Y (2006) Removal of Congo red from aqueous solution by adsorption onto acid activated red mud. J Hazard Mater 138: 409–415

Veli, S. and Aly, B. (2007) Adsorption of copper and zinc from aqueous solutions by using natural clay. **149**, 226–233

Vig K, Megharaj M, Sethunathan N, Naidu R (2003) Bioavailability and toxicity of cadmium to microorganisms and their activities in soil: a review. Adv Environ Res 8:121–135

Xu, L., Zheng, X., Cui, H., Zhu, Z., Liang, J., and Zhou, J. (2017) Equilibrium, kinetic, and thermodynamic studies on the adsorption of cadmium from aqueous solution by modified biomass ash. **2017**. Hindawi Publishing Corporation